Raman intensity profiles of folded longitudinal phonon modes in SiC polytypes

S. Nakashima*
Department of Electrical and Electronics Engineering, Miyazaki University, 1-1 Gakuen-Kibanadai-Nishi, Miyazaki 889-2192, Japan

H. Harima
Department of Applied Physics, Osaka University, 2-1 Yamadaoka, Suita, Osaka 565-0871, Japan

T. Tomita and T. Suemoto
The Institute for Solid State Physics, The University of Tokyo, 5-1-5 Kashiwanoha, Kashiwa, Chiba 277-8581, Japan
(Received 3 August 2000)

Raman spectral profiles of folded longitudinal phonon modes in $4H$-, $6H$-, and $21R$- SiC polytypes which form natural superlattices have been studied experimentally and theoretically. The Raman intensity of the folded longitudinal modes is very weak except for the mode corresponding to a zone-center phonon mode in the $3C$ polytype. The intensity profiles of these modes are interpreted on the basis of the bond polarizability concept when one takes into account difference of the bond Raman polarizability between the cubic and hexagonal environments. The agreement of the measured and calculated intensities indicates that the bond polarizability model can be applied to Raman spectral profiles of the longitudinal folded modes as well as transverse folded modes in SiC.

I. INTRODUCTION

It is well known that SiC has a large number of polytypes which form natural superlattices. Long period SiC polytypes show a various number of Raman bands.[1–4] These Raman bands originate from the zone folding of transverse (longitudinal) acoustic and optical branches along the $\langle 111 \rangle$ direction in the $3C$ polytype with zinc-blende structure. The dispersion curves of transverse phonons propagating along the $\langle 111 \rangle$ direction axis in the $3C$ polytype have precisely been determined from the frequencies of observed folded modes in various polytypes.[3,4] The Raman intensity profiles of the folded transverse acoustic (FTA) and optical (FTO) branches are well reproduced by the spectra calculated on the basis of the bond polarizability concept and one-dimensional lattice dynamics model.[3] The analysis of the Raman intensity profiles of the folded modes has enabled us to identify the stacking structures of Si-C double atomic layers in long period SiC polytypes.[5]

The Raman intensity profiles have also been studied on the basis of the bond polarizability model of IV group semiconductors,[6,7] artificial superlattices (SL's) such as GaAs-AlAs SL's,[8–12] other SL's,[13–16] fullerenes,[17–19] IV-IV group SL's,[20–22] and layered compounds.[23,24] The Raman spectra calculated based on the bond polarizability model reproduce well the observed ones for various crystals.

The folded modes of the longitudinal optical (FLO) and acoustic branches (FLA) were also observed in SiC polytypes and the dispersion curves of the LO and LA modes in the $3C$ polytype were deduced.[4] The Raman intensities of these modes except an unfolded optical mode at ~ 796 cm^{-1} which corresponds to the phonon at the Γ point in $3C$ polytype are very weak as compared with those of the folded transverse (FT) modes. The weak intensity of the folded longitudinal (FL) modes may be due to reduction of the polarization in a unit cell by partial cancellation of the bond polarizabilities.

Since SiC is a polar crystal, the polarization fields associated with longitudinal vibrations should contribute to the phonon dispersion and the Raman intensity. The Raman scattering efficiency of the LO modes is related to two terms; the contributions from the short-range field $(\delta\chi/\delta u)$ and long-range field $(\delta\chi/\delta E)$,[25] where χ is the electronic susceptibility, u is the atomic displacement, and E is the electric field. For crystals with the zinc-blende structure, the Raman tensor component of the LO mode incorporating the latter contribution is related to that of TO phonons by the following equation:

$$\frac{d_{\mathrm{LO}}}{d_{\mathrm{TO}}} = \left(1 - \frac{\omega_{\mathrm{LO}}^2 - \omega_{\mathrm{TO}}^2}{C\omega_{\mathrm{TO}}^2}\right), \tag{1}$$

where d is the tensor component and ω_{TO} and ω_{LO} are the frequencies of the TO and LO modes, respectively. C is the so-called Faust-Henry coefficient given by

$$C = e^*(\delta\chi/\delta u)[m\omega_{\mathrm{TO}}^2(\delta\chi/\delta E)]^{-1}, \tag{2}$$

where e^* is the effective charge associated with the optical phonons and m is their reduced mass. The Faust-Henry coefficient of various zinc-blende-type semiconductors was experimentally determined from the intensity ratio of the LO and TO modes.[25]

While the Raman intensity analysis of the LO modes has been made on the zinc-blende structure, little is known about the LO modes in other structures. We have tried to examine whether the incorporation of the long-range field into the bond Raman polarizability is allowed for uniaxial SiC polytypes which have a large number of longitudinal modes.

SiC polytypes except $3C$ and $2H$ polytypes are constructed from mixture of cubic and hexagonal stackings of a Si-C double layer. So far, the intensity profiles of the FTO

 ©2000 The American Physical Society

and FTA modes were calculated assuming that the bond polarizabilities for bonds in cubic and hexagonal environments are the same but the force fields are different.[3] However, this assumption does not well explain the observed spectral profiles of the FLO and FLA modes. This fact may indicate that the bond Raman polarizability relevant to the folded longitudinal modes differs for the bonds in different environments. It is of interest to examine the influence of local atomic arrangement on the bond Raman polarizabilities of the longitudinal modes, because it will provide information on the structure dependence of the dielectric properties in SiC polytypes.

In the present work, we have analyzed the intensity profiles of the FL modes in SiC polytypes based on the bond polarizability concept. The Raman intensity profiles of the folded longitudinal modes are calculated taking into account difference of forces and bond polarizabilities for the environments. The calculated Raman intensity profiles are compared with observed spectral profiles for $4H$, $6H$, $15R$, and $21R$ polytypes. Discussion is given for the bond polarizability approach.

II. EXPERIMENTAL RESULTS

A. Experiment

Polytype samples used in this experiment were single crystals prepared by the Acheson method or a chemical deposition method. The frequencies of the folded modes were measured using $4H$, $6H$, $15R$, $27R$, $33R$, $51R$ polytypes. The intensity profiles of the FL modes were precisely measured for $4H$, $6H$, $15R$, and $21R$ polytypes. Raman spectra were measured at room temperature using the 488-nm line of an Ar laser. The phonon Raman spectra show no remarkable resonance enhancement for the laser light with wavelengths from 456.5 to 514.5 nm. A quasiback scattering geometry was employed for the (0001) face. For this configuration the A-symmetry phonon modes propagating along the c direction are observed. The scattered light was dispersed by a double monochromator with $f=0.85$ m and detected by a cooled CCD (charge-coupled device) detector. The carrier concentration of the samples used was less than $5\times10^{16}\,\mathrm{cm}^{-3}$.

B. Intensity profiles of FLO and FLA modes

Raman-scattering spectra of various polytypes have been measured at room temperature. The results for three typical polytypes are shown in Fig. 1. The FL modes in the figures are labeled by $x=q/q_{\max}$, where x is the reduced wave vector of the corresponding phonon modes in $3C$ polytype.[3] As shown in this figure, the folded LO and LA modes are very weak except for the FLO(0) mode (unfolded mode). The intensities of the FL mode relative to that of the FLO ($x=0$) mode lies in a range of 10^{-2}–10^{-4} (Tables I and II). As shown in Fig. 1(a), the FL(2/6), FL(6/6) modes in the $6H$ polytype are not observed because these modes are Raman inactive B_1 modes. For the $15R$ polytype the FLA(4/5) doublet at 568.6 and 573.4 cm^{-1} is clearly seen [Fig. 1(b)].

The FLO(2/7) modes in the $21R$ polytype are very weak and their intensity relative to that of FLO(0) mode is less than 10^{-5}, but the traces are found at 940 and 949 cm^{-1}. For the $21R$ polytype, the Raman intensity relative to that of the FLO(0) mode is the largest for the FLO(4/7) mode and weak for the FLO(2/7) and FLO(6/7) modes as shown in Fig. 1(c) and Table II. It is to be noted that the width of the FLO modes and especially the FLA modes is small, being about 1 cm^{-1} for the FLA modes and about 2 cm^{-1} for FLO modes. This implies that there are no dominant decay channels into two-acoustic phonon modes unlike high-frequency optic modes.

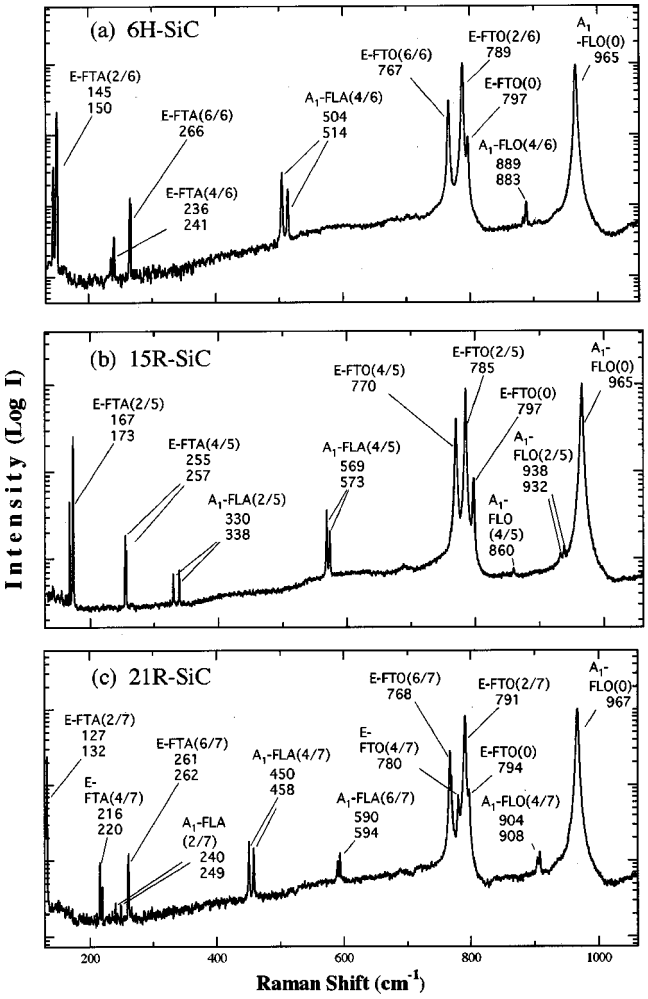

FIG. 1. The whole Raman spectra of (a) $6H$-, (b) $15R$-, and (c) $21R$-SiC crystals. The intensity is plotted on log scale.

C. Dispersion curves of the LO and LA branches of $3C$ SiC

We have also observed the FL modes for various polytypes. The dispersion curves of the longitudinal acoustic and optical phonons propagating along the $\langle 111\rangle$ direction in the $3C$ polytype are derived from the frequencies of the FL modes, in various polytypes.[4] The result is shown in Fig. 2. The frequencies of the folded modes in α-SiC polytypes do not much deviate from the dispersion curves of $3C$ SiC.

The frequency of the unfolded LO mode depends slightly on the polytype. Hofmann *et al.*[26] have suggested that the frequency decreases with increase of the hexagonality. However, we did not found any remarkable polytype dependence of the frequency for the FLO(0) modes. For example, the frequency of the A_1(LO) mode in $6H$-SiC (964.2 ± 0.2) is almost the same as that of the $4H$ polytype (964.2 ± 0.2).[27]

TABLE I. Raman intensity of the FLO and FLA modes in 6*H*-SiC polytype. The measured intensities are compared with ones calculated using parameters in Table III.

6*H* SiC	FLA			FLO		
$x=q/q_M$	ω (cm^{-1})	$I/I_{\mathrm{LO}}(0)$	Calc.	ω (cm^{-1})	$I/I_{\mathrm{LO}}(0)$	Calc.
0				965	1.0	1.0
2/6						
4/6	513.9	7.6×10^{-3}	8.8×10^{-3}	889	4.3×10^{-3}	2.5×10^{-3}
	504.6	1.3×10^{-2}	1.0×10^{-3}	883[a]	~0	1.9×10^{-3}
6/6						

[a]Observed in resonance condition using 302-nm line.

III. CALCULATION OF THE INTENSITY PROFILES OF THE FLO AND FLA MODES

A. Bond polarizability approach to the Raman intensity

The Raman tensor component of the LO phonons is associated with that of the TO phonon via the Faust-Henry coefficient. The use of the renormalized bond Raman polarizability may be allowed for the FLA and FLO modes corresponding to the modes with wave vectors inside and at the edge of the basic Brillouin zone of the 3*C* polytype when we assume that the common Faust-Henry coefficient[24] can be used for these modes.

The Raman intensity of the λth mode is given by

$$W_\lambda = S[n(\omega)+1]\omega^{-1}\Sigma[\mathbf{e}_i\boldsymbol{\alpha}'(\lambda)\mathbf{e}_s]^2, \tag{3}$$

where S is a constant of proportionality, ω is the frequency of the phonon mode, $n(\omega)$ is the Bose factor, and $\mathbf{e}_i$ and $\mathbf{e}_s$ are the polarization vectors of the incident and scattered light, respectively. In Eq. (3) the Raman polarizability $\boldsymbol{\alpha}'(\lambda)$ consists of the bond Raman polarizabilities which include the contribution from the polarization field.

In all SiC polytypes, any Si or C atom has the same first-neighbor environment and the difference arises in the next-nearest neighbors and higher neighbors. The unit cell of polytypes consists of Si-C double layers and the different structures of SiC result from different stackings of the Si-C double layers. For the 3*C* polytype (β-SiC), all the double layers occur in a cubic environment, and for the 2*H* polytype all the double layers occur in a hexagonal environment. Other polytypes are constructed from mixtures of the cubic and hexagonal stackings. The atomic distances are almost the same for the different polytypes and the dependence of the atomic distance on the polytype structure is very weak.[28]

For the axial A_1-type modes, the bonds in SiC polytypes are classified into two groups: (i) the bonds inclined to the *c* axis (inclined bond) and (ii) the bond parallel to the *c* axis (parallel bond). The bond Raman polarizability tensors calculated are shown in Fig. 3, where $\alpha_\parallel$ and $\alpha_\perp$ are the parallel and perpendicular components of the bond polarizability, respectively. For the axial (A_1-type) mode, the inclined bonds in groups (i)a and (i)b make the same contribution to the tensor components, although they have different signs for the *E*-type transverse phonons.[28,3] The parallel bonds contributes only to the diagonal components of the Raman tensors. For a back scattering geometry using the *c* face of SiC, *xx* or *yy* component of the Raman tensor contributes to the Raman intensity of the axial (A_1-type) modes. The Raman polarizability tensor for axial vibration is expressed as

$$\begin{aligned}\alpha_{\rho\rho}(\lambda) &= \Sigma\,\alpha^{(a)}_{\rho\rho}[A^a_\lambda(z_i)-A^a_\lambda(z_{i+1})] \\ &\quad+\Sigma\,\alpha^{(c)}_{\rho\rho}[A^c_\lambda(z_i)-A^c_\lambda(z_{i+1})] \\ &= \mathrm{I}(\alpha^{(a)}_{\rho\rho})+\mathrm{II}(\alpha^{(c)}_{\rho\rho}).\end{aligned} \tag{4}$$

For the FT modes, the bond Raman polarizability $\alpha^{(a)}_{\rho\rho}$ was taken to be the same for cubic and hexagonal environments.[3] In the case that $\alpha^{(a)}_{\rho\rho}$ does not depend on the environment, the first term in Eq. (4) is reduced to

$$\mathrm{I}(\alpha_{\rho\rho}) = \alpha^{(a)}_{\rho\rho}\Sigma[A^a_\lambda(z_i)-A^a_\lambda(z_{i+1})], \tag{5}$$

where $A^a(z_i)-A^a(z_{i+1})$ and $A^c(z_i)-A^c(z_{i+1})$ are the relative displacement of the atomic planes connected by bonds

TABLE II. Raman intensity of the FLO and FLA modes in 21*R*-SiC polytype. The measured intensities are compared with ones calculated using parameters in Table III.

21*R*-SiC	FLA			FLO		
$x=q/q_M$	ω (cm^{-1})	$I/I_{\mathrm{LO}}(0)$	Calc.	ω (cm^{-1})	$I/I_{\mathrm{LO}}(0)$	Calc.
0				966.7	1.0	1.0
2/7	249.1	3.4×10^{-3}	1.9×10^{-3}	$\sim$949	$<10^{-5}$	1.6×10^{-3}
	240.3	4.4×10^{-4}	3.3×10^{-3}	$\sim$940	$<10^{-5}$	1×10^{-4}
4/7	457.5	4.6×10^{-3}	5.8×10^{-3}	907.8	3.4×10^{-3}	1.9×10^{-3}
	449.9	6.3×10^{-3}	0.9×10^{-4}	904.2	3.0×10^{-3}	1.4×10^{-3}
6/7	593.5	2.8×10^{-3}	1.6×10^{-3}	850.1	3.2×10^{-3}	1.3×10^{-3}
	590.0	1.2×10^{-3}	2.6×10^{-3}	840.1	7.3×10^{-4}	3.3×10^{-4}

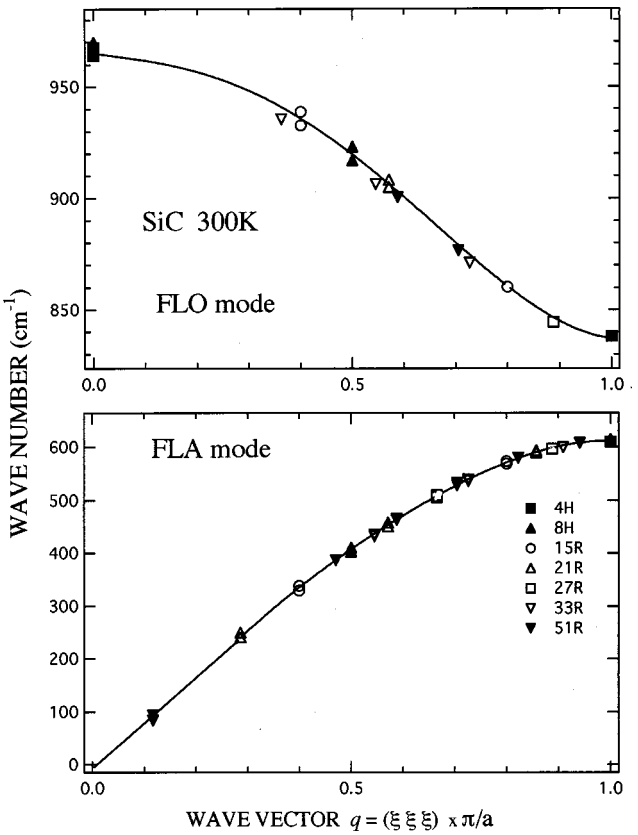

FIG. 2. Dispersion curves of the LO and LA modes which propagate along the ⟨111⟩ direction in 3*C*-SiC, which are estimated from the frequencies of the observed folded modes in various polytypes.

inclined and parallel to the *c* axis, respectively. The summation is taken over a unit cell. The phase of the relative displacement of a double planes $[A^q_\lambda(z_i)-A^q_\lambda(z_{i+1})]$ differ by $2m\pi/n$ from that of the neighboring double planes, where n is the number of the Si-C double planes in the unit cell, and $|m|\leqslant n/2$). Accordingly, in Eq. (5) these displacements canceled each other out. As a result, the first term of Eq. (4) becomes almost zero. The same argument can be applied to the second term. However, provided that $\alpha^{(c)}_{\rho\rho}$ differs for cubic and hexagonal environments, the second term gives a finite value, although it is small.

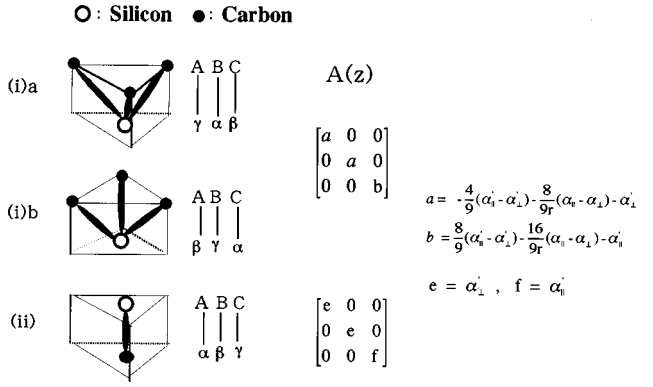

FIG. 3. The bondings in SiC polytypes are classified into two groups. The bond Raman polarizability tensors when assuming a zinc-blende structure are shown for the A_1-type phonon modes.

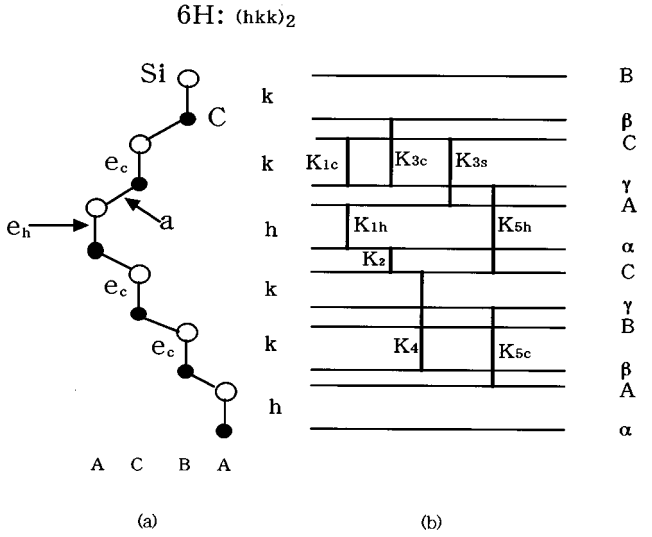

FIG. 4. The stacking arrangement of the 6*H* polytype is depicted in (a). One-dimensional lattice dynamics model of SiC for the longitudinal modes and the force-constant parameters are shown in (b).

Let us assume that, for the FL modes, the bond Raman polarizability depends on the stacking only for the parallel bonds as shown in Fig. 4(a). The parallel bond in group (ii) will play a dominant role for the Raman intensity of the A_1-type FLO and FLA phonons, because the bond stretching occurs for this bond. On the other hand, for the Raman intensity of the FTA and FTO modes, the contribution from the bonds in groups (i)a and (i)b is dominant and even a stacking independent bond polarizability model gave a good agreement between the experimental and calculated results.[3] Under the above assumption the Raman polarizability of the λth FLO or FLA mode is reduced to the following form:

$$\alpha_{\rho\rho}(\lambda)=a\Sigma[A^a_\lambda(z_i)-A^a_\lambda(z_{i+1})]+\Sigma e(j)[A^c_\lambda(z_i)-A^c_\lambda(z_{i+1})], \tag{6}$$

where we put

$$e(j)=e_c \text{ for the cubic environment,}$$

and

$$e(j)=e_h \text{ for the hexagonal environment.}$$

B. One-dimensional lattice dynamics model

The displacements of the atomic planes for the folded transverse (FT) modes have so far been calculated using a one-dimensional lattice dynamics model.[3,28] The Raman intensity of the FT modes depends strongly on the displacement pattern of the atomic planes.[3,29] We have calculated the displacements for the FL modes using a lattice dynamics model similar to that of the FT modes.[3] The displacement amplitudes of the atomic planes are obtained as solutions of the equations of motion,

$$M_j\omega^2 u(n|j)=\sum_{r,s} D^r_{j,j+s}u(n+r|j+s), \tag{7}$$

where $u(n|j)$ and M_j are the displacement and mass of the jth rigid plane in the nth unit cell, respectively, and $D^r_{j,j+s}$ is the interplanar force constant. We look for solutions of the exponential form,

$$u(n|j)=u(j)\exp(-iqz_n),\quad u(j)=A_j\exp[i\phi(j,q)], \quad (8)$$

and $\phi(j,q)=-q_jz_j+\phi_j(q)$.

In the Raman intensity calculation we use the normalized displacement amplitudes.

The frequency of the folded phonon modes are determined from the secular equation,

$$|M_j\omega^2\delta_{ij}-D_{ij}(q)|=0. \quad (9)$$

where

$$D_{ij}=\exp[-iq(z_j-z_i)]\Sigma\,\delta^n_{i,j}\exp(-iqz_n). \quad (10)$$

The Si-C bond chain and the force parameters for the 6H polytype are shown in Figs. 4(a) and 4(b). The 6H polytype contains two hexagonal and four cubic stackings in the unit cell. The interplanar forces are taken into account up to the third-neighbor planes. The force constants and bond Raman polarizabilities have been determined so that the calculated phonon dispersions for the $3C$ polytype, the splitting of the FLA modes and also the Raman intensity profile fit to the experimental results. The force-constant parameters thus determined are listed in Table III. These parameters reproduce well the dispersion curves of the LO and LA phonon modes propagating along the $\langle 111\rangle$ direction of the $3C$ polytype. The dispersions are not so sensitive to the choice of the parameters. The dispersion curves calculated using the parameters in Table III is almost the same as those shown in Ref. 4, though the third-neighbor forces were not included in Ref. 4. Calculated frequencies of the FLO(0) modes in $4H$, $6H$, $15R$, and $21R$ polytypes do not show clear hexagonality dependence contrary to the suggestion of Hofmann.[26]

IV. DISCUSSION

The calculated intensity of the FLO and FLA modes is compared with the observed spectral profiles in Fig. 1, where their intensity is normalized for that of each FLO(0) mode. In this calculation we take $qc=0.017$, which corresponds to the 488-nm excitation. As shown in Tables I and II, the qualitative agreement is obtained on the whole, though there are some discrepancies in certain modes. The result of the fitting reveals that it is necessary to take into account the difference between the bond polarizabilities for the cubic and hexagonal environments to reproduce the observed profiles.

Figure 5 shows Raman intensity of the FLA(4/4) mode in $4H$-SiC and the FLA(6/7) modes in $21R$ SiC against the bond-Raman-polarizability ratio e_h/e_c. The horizontal arrows denote the experimental intensity. Here, we assume that $e_h>e_c$. This figure shows that about ten percent difference of the two polarizabilities is needed to reproduce the Raman profiles of the FL modes. The best fit value of the ratio e_h/e_c is 1.11 for the FLA (4/4) mode in $4H$-SiC, 1.14 for the FLA(6/7+) mode at 593.5 cm^{-1} and 1.08 for the FLA(6/7−) mode at 590 cm^{-1}. We take $e_h/e_c=1.10$ for the bond polarizability ratio e_h/e_c in all the polytypes (Table III). In Tables I and II we compare the calculated and experimental intensities of the FL modes in $6H$ and $21R$ polytypes.

TABLE III. Force-constant parameters and bond Raman polarizabilities.

K_{1c}	K_{1h}	K_2	K_{3c}	K_{3s}	K_4	K_{5c}	K_{5h} (10^4 dyn/cm)	e_c/a	e_h/a
14.8	14.2	32	−2.0	11	−0.25	−0.4	0.25	0.69	0.76

It is well known that the Raman intensity is generally larger for covalent crystals than ionic crystals in which electrons are localized at around nucleus. In the framework of the bond polarizability model, the Raman polarizability, i.e., the derivative of the bond polarizability with the atomic displacement is considered to be large for covalent bonding. The charge density distribution in SiC polytypes has been discussed by several authors. Park *et al.* have calculated valence charge density for $3C$, $2H$, $4H$, and $6H$ polytypes.[30] Their result shows that the charge distributions are slightly different for the hexagonal and cubic environments. According to their calculation, the hexagonal layers of $4H$-SiC are positively charged while the cubic layers are negatively charged as compared with that of $3C$ structure. From studies of the chemical shift for several SiC polytypes, Sorokin *et al.* concluded that the average charge on Si atoms vary with the hexagonality.[31] The similar conclusion was obtained by Guth and Petuskey,[32] though their dependence is weaker than the result of Sorokin *et al.*[3] According to the calculation by Park *et al.*, the valence charge density for parallel bonds within the Si-C bilayer is slightly positive for the hexagonal environments as compared with that of the cubically stacked bilayer. Their result seems to indicate that the ionic character is large for hexagonal environment. The bond charge in the SiC polytypes has also been discussed by Qteish *et al.*[33] and K. Karch *et al.*,[34] but quantitative analysis on the hexagonality dependence has not yet been made. From the above discussion it is likely that the bond polarizability of the parallel bonds is larger in the cubic environment than in the hexagonal environment. This consideration, however, does not necessarily lead to the conclusion that e_c is larger than e_h, because the bond Raman polarizability is complex functions of the bond polarizability components $\alpha_\parallel$ and $\alpha_\perp$ and these derivatives. In the present work we assume that e_h is larger than e_c. The same assumption has been made in the resonant Raman scattering of the FL modes in SiC.[35] As shown in Fig. 5, the Raman intensity profile of the FL modes does not depend on the absolute magnitudes of e_h and e_c, but on their difference. It is to be noted that the sign and relative magnitude of the Raman polarizabilities e_c and e_h cannot be directly determined from the analysis of the observed Raman profiles, because the Raman intensity is related to the square of the Raman polarizability. It is instructive to compare the Raman spectra of the folded longitudinal and transverse modes. In the framework of the bond polarizability treatment, the parallel bond does not contribute to the Raman polarizability for the FTA and FTO modes, because the two atoms at the edge of this bond move perpendicularly to the bond. On the contrary, the stretching motion of the parallel bond will contribute largely to the Raman polarizability of the FLA and FLO mode. As stated before, the bond Raman polarizability treatment quantitatively explains the spectral

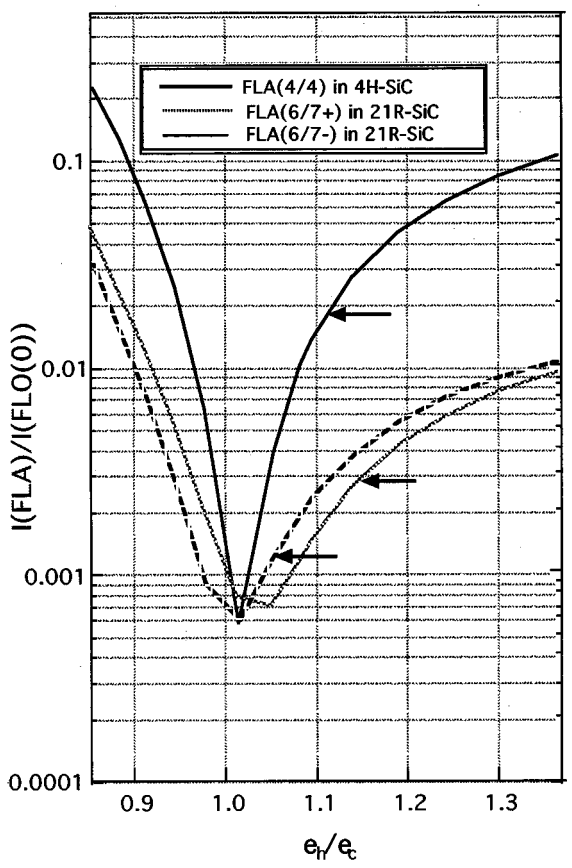

FIG. 5. Calculated Raman intensity as a function of the bond Raman polarizability ratio of e_c and e_h, where e_h/a is taken to be 0.76. The horizontal arrows show the experimental Raman intensity. The + and − modes denote the upper and lower frequency components in the FLA doublets.

profiles for the FTA and FTO modes, although the stacking dependence of the bond Raman polarizability for the inclined bonds was neglected. This fact together with the results of the present work suggests that the local stacking structure has a striking influence on the bond Raman polarizability of the parallel bond. The polarization field associated with the longitudinal modes is isotropic and might not contribute to the difference of the bond Raman polarizabilities in the cubic and hexagonal environments.

It is of interest to compare the Raman intensity of the FLA modes for artificial superlattices such as GaAs-AlAs system and natural superlattices, SiC polytypes. The relative Raman intensity of the FLA modes in GaAs-AlAs superlattices is strong compared with the FLA modes of SiC polytypes. The reason for the difference is that in SiC the bond Raman polarizabilities are nearly equal for different stacking layers, but in GaAs-AlAs superlattices the bond Raman polarizabilities are much different for AlAs and GaAs layers. The difference in the bond polarizabilities at the interface of the constituent layers contributes mainly to the Raman intensity for GaAs-AlAs superlattices, while in SiC the bond Raman polarizabilities cancel each other out.

V. CONCLUSION

In the present work, we have analyzed the Raman intensity profiles of the FLO and FLA modes in SiC polytypes using the bond polarizability approach, in which the term $(\delta\chi/\delta E)$ is incorporated into the bond Raman polarizability. A reasonable agreement is obtained for the experimental and calculated Raman profiles for these modes, although the effect of the long-range field on the Raman intensity is not directly taken into account. The force constant parameters and bond Raman polarizabilities are determined so as to fit the frequency and the Raman intensity. These parameters are universal ones and can be applied to any other SiC polytypes. This fact suggests that the bond polarizability approach is useful to examine the Raman intensity for the longitudinal phonon modes which accompany long-range polarization field in SiC. It is found that it is necessary to take into consideration the difference in the forces and bond Raman polarizabilities of the parallel bonds between cubic and hexagonal stackings in order to explain the Raman intensity profiles of FLO and FLA modes in SiC polytypes. The investigation of the Raman intensity using the bond Raman polarizabilities will provide a clue for completely consistent description of the lattice polarization and charge distribution in the SiC polytype system.

*Electronic address: nakashim@pem.miyazaki-u.ac.jp

[1] D. W. Feldman, J. H. Parker, Jr., W. J. Choyke, and L. Patrick, Phys. Rev. **173**, 787 (1968).
[2] S. Nakshima, H. Katahama, Y. Nakakura, and A. Mitsuishi, Phys. Rev. B **33**, 5721 (1986).
[3] S. Nakashima and K. Tahara, Phys. Rev. B **40**, 6339 (1989).
[4] S. Nakashima and H. Harima, Phys. Status Solidi A **162**, 39 (1997).
[5] S. Nakashima, K. Kisoda, and J.-P. Gauthier, J. Appl. Phys. **75**, 5354 (1994).
[6] R. Tubino and L. Piseri, Phys. Rev. B **11**, 5145 (1975).
[7] S. Go, H. Bilz, and M. Cardona, Phys. Rev. Lett. **34**, 580 (1975).
[8] B. Zhu and K. A. Chao, Phys. Rev. B **36**, 4906 (1987).
[9] S. Nakashima, K. Tahara, M. Hangyo, and M. Nakayama, Phys. Rev. B **41**, 5221 (1990).
[10] P. Castrillo, G. Armelles, L. Gonzalez, P. S. Dominguez, and L. Colombo, Phys. Rev. B **51**, 1647 (1995).
[11] M. P. Halsall and P. Dawson, J. Appl. Phys. **81**, 224 (1997).
[12] P. Casterillo, G. Armelles, and J. Barbolla, Solid State Commun. **98**, 307 (1996).
[13] G. Wei, J. Zi, K. Zhang, and X. Xie, J. Appl. Phys. **82**, 622 (1997).
[14] J. Zi, G. Wei, K. Zhang, and X. Xie, J. Phys. C **8**, 6329 (1996).
[15] M. I. Allonso, P. Castrillo, G. Armelles, A. Ruiz, M. Recio, and F. Briones, Phys. Rev. B **45**, 9054 (1992).
[16] R. Sugie, H. Ohta, H. Harima, S. Nakashima, and H. Fujiyasu, J. Appl. Phys. **80**, 5946 (1996).
[17] S. Guha, J. Menéndes, J. B. Page, and G. B. Adams, Phys. Rev. B **53**, 13 106 (1996).
[18] D. W. Snoke, M. Cardona, S. Sanguinetti, and C. Benedek, Phys. Rev. B **53**, 12 641 (1996).
[19] D. W. Snoke and M. Cardona, Solid State Commun. **87**, 121 (1993).
[20] M. W. C. Dharma-Wardana, G. C. Aers, D. J. Lockwood, and

J.-M. Baribeau, Phys. Rev. B **41**, 5319 (1990).
[21] J. Spitzer, T. Ruf, M. Cardona, W. Dondle, R. Schorer, G. Abstreiter, and E. E. Haller, Phys. Rev. Lett. **72**, 1565 (1994).
[22] M. A. Araújo Silva, E. Ribeiro, P. A. Schulz, F. Cerdeira, and J. C. Bean, Phys. Rev. B **53**, 15 871 (1996).
[23] S. Nakashima, H. Katahama, Y. Nakakura, A. Mitsuishi, and B. Palosz, Phys. Rev. B **31**, 6531 (1985).
[24] S. Nakashima and M. Balkanski, Phys. Rev. B **34**, 5801 (1986).
[25] M. Cardona, *Light Scattering in Solids II*, edited by M. Cardona and G. Güntherodt (Springer, Berlin, 1982), Chap. 2.
[26] M. Hofmann, A. Zywietz, K. Karch, and F. Bechstedt, Phys. Rev. B **50**, 13 401 (1994).
[27] H. Harima, S. Nakashima, and T. Uemura, J. Appl. Phys. **78**, 1996 (1995).
[28] S. Nakashima, H. Katahama, Y. Nakakura, and A. Mitsuishi, Phys. Rev. B **33**, 5721 (1986).
[29] S. Nakashima, Y. Nakakura, A. Wada, and K. Kunc, J. Phys. Soc. Jpn. **57**, 3828 (1988).
[30] C. H. Park, R-H. Cheong, K-H. Lee, and K. J. Chang, Phys. Rev. B **49**, 4485 (1994).
[31] N. D. Sorokin, Y. M. Tairov, V. F. Tsvetkov, and M. A. Chernov, Dokl. Akad. Nauk (SSSR) **267**, 1380 (1982) [Sov. Phys. Dokl. **27**, 170 (1982)].
[32] J. Guth and W. T. Petuskey, J. Phys. Chem. Solids **48**, 541 (1987).
[33] A. Qteish, V. Heine, and R. J. Needs, Phys. Rev. B **45**, 6534 (1992).
[34] K. Karch, P. Pavone, W. Windl, O. Schutt, and D. Strauch, Phys. Rev. B **50**, 17 054 (1994).
[35] T. Tomita, S. Saito, M. Baba, M. Hundhausen, T. Suemoto, and S. Nakashima, Phys. Rev. B **62**, 12 896 (2000).